VOLUME 03 ISSUE 02 (2024)

AMERICAN JOURNAL OF LIFE SCIENCE AND INNOVATION (AJLSI)

ISSN: 2833-1397 (ONLINE)

PUBLISHED BY
E-PALLI PUBLISHERS, DELAWARE, USA

American Journal of
Life Science and Innovation (AJLSI)

Volume 3 Issue 2, Year 2024
ISSN: 2833-1397 (Online)
DOI: https://doi.org/10.54536/ajlsi.v3i2.4281
https://journals.e-palli.com/home/index.php/ajlsi

Evaluation of the Antifungal Effect of Green Synthesized Metal Oxide Nanoparticles Against Plant Pathogenic *Rhizoctonia* Species

H. K. S. Madusanka[1*], A. G. B. Aruggoda[1], J. A. S. Chathurika[2], S. R. Weerakoon[3]

Article Information

Received: November 08, 2024

Accepted: December 10, 2024

Published: December 15, 2024

Keywords

Antifungal Activity, Green-Synthesized Nanoparticles, Poisoned Food Technique, Rhizoctonia Species

ABSTRACT

The current study successfully synthesized zinc oxide (ZnO), copper oxide (CuO), and iron oxide (FeO) nanoparticles (NPs) using cost-effective and environmentally friendly procedures. The synthesized NPs were characterized by UV-Vis spectroscopy and SEM analysis. UV-Vis spectroscopy revealed characteristic absorption peaks at 356 nm for ZnO NPs, confirming their synthesis. SEM analysis showed a heterogeneous distribution of nanoparticle sizes, with ZnO NPs averaging 81 nm, CuO NPs averaging 108 nm, and FeO NPs averaging 82 nm. The antifungal activity of the synthesized nanoparticles was evaluated at various concentrations using the poisoned food technique. The results indicated a dose-dependent inhibition of mycelial growth by ZnO and CuO NPs, with higher concentrations (500 and 1000 mg/L) showing significant inhibition compared to untreated *Rhizoctonia* species. Specifically, CuO NPs exhibited mycelial growth inhibition percentages of 70.64% and 73.43% at 500 and 1000 mg/L, respectively, while ZnO NPs showed inhibition percentages of 78.38% and 80.94% at the same concentrations. Statistical analysis using one-way ANOVA revealed significant differences among the treatment groups ($p < 0.001$). In contrast, FeO NPs did not exhibit a dose-dependent inhibition of mycelial growth but showed a minor, statistically insignificant promotion. Among the tested NPs, CuO NPs at 1000 mg/L achieved the highest inhibition, followed by ZnO NPs. The observed variations in mycelial inhibition by different nanoparticles at various concentrations underscore the complexity of nanoparticle-pathogen interactions and highlight the need for further research to optimize their antifungal efficacy.

INTRODUCTION

The *Rhizoctonia* genus belongs to the Basidiomycete phylum and consists of anamorphic fungi with different teleomorphs (Moliszewska *et al.*, 2023). *Rhizoctonia* spp. is a significant plant pathogenic fungus responsible for diseases such as wilt and root rot. These diseases can manifest during the seedling stage as well as in the later stages of crop growth, leading to early infections that often result in plant death (Jaiswal *et al.*, 2014). *R. solani* produces numerous enzymes and phytotoxic substances that contribute to its pathogenicity, causing specific fungal disease symptoms in crops (Mousa *et al.*, 2024). The *Rhizoctonia* genus comprises a vast and diverse group of soil-dwelling fungi, including binucleate *Rhizoctonia*. While many species within this genus are plant pathogens and typically polyphagous, they exhibit distinct pathogenic preferences for specific plant species. Despite their broad and varied host range, their affinity for certain plants is individually determined. Among them, *Rhizoctonia solani* is the most commonly reported and is recognized as a significant plant pathogen (Moliszewska *et al.*, 2023).

The current research aims to investigate the antifungal potential of green-synthesized nanoparticles, including ZnO, CuO, and FeO NPs, against *Rhizoctonia* species. The study will involve synthesizing the nanoparticles using green methods and characterizing their physicochemical properties. Antifungal activity will be evaluated over a range of concentrations (0, 50, 100, 500, and 1000 mg/L) using the poison food technique to determine inhibition effects.

LITERATURE REVIEW

Rhizoctonia spp cause significant damage to agricultural crops cuasing several diseases. Sheath blight, caused by *Rhizoctonia solani*, is a significant challenge for rice farmers, leading to yield losses ranging from 25% to 50% (Chowdhury *et al.*, 2019). *Rhizoctonia* species are responsible for several diseases across different crops: soybeans suffer from aerial blight and web blight, tomatoes are susceptible to soil rot and fruit rot, peppers are affected by damping-off, and eggplants are prone to brown spot (Tu *et al.*, 1996).

Disease management for *Rhizoctonia* spp is done by Cultural Practices and Fungicides. Cultural practices includes Select cultivars that are resistant, tolerant, or less susceptible to *Rhizoctonia* diseases, purchase certified disease-free seed or disease free transplants, crop rotation etc. Although cultural approache is most essential control strategy, chemical management is still an important tool to decrease *R. solani* (Tsror, 2010). As chemical management, applying Pentachloronitrobenzene-based fungicides , Tebuconazole, carbendazim, iprodione, and

[1] Department of Agricultural and Plantation Engineering, The Open University of Sri Lanka, Nawala, Nugegoda, Sri Lanka
[2] Department of Urban Bio-resources, University of Sri Jayawardanapura, Ganagodawila, Nugegoda, Sri Lanka
[3] Department of Botany, The Open University of Sri Lanka, Nawala, Nugegoda, Sri Lanka
[*] Corresponding author's e-mail: hksma@ou.ac.lk

chlorothaloniland systemic fungicides such as carboxin, triadimefon, and thiophanate-methylis effective against *Rhizoctonia* (Karkee & Mandal, 2020; Chaube & Pundhir, 2005).

The growing concern over alternative approaches to chemical management of pathogenic fungi is closely linked to soil and environmental health. This includes issues such as increased pesticide residues in soil and water bodies, reduction in beneficial soil organisms, changes in soil physical and chemical properties, and pesticide resistance in pathogens (Sharma *et al.*, 2019). Chemical control is the most widely used method to manage soilborne fungal pathogens. However, the negative environmental and health effects, disruption of natural ecosystem balance, and the emergence of fungal resistance to chemical pesticides highlight the need for sustainable and cost-effective alternatives. Research has demonstrated that nanoparticles show promise as effective antimicrobial agents and biosensors for detecting plant pathogens, particularly against soil-borne varieties, offering a comparatively environmentally friendly solution (Dutta *et al.*, 2023). Nanoparticles smaller than 100 nm possess a higher surface area to volume ratio and enhanced reactivity, which enhances their suitability for widespread application in both human and plant pathology (Jeevanandam *et al.*, 2018).

MATERIALS AND METHODS

Biologic Material and Chemical Reagents

Fresh samples of *S. molesta* and *Mimosa pigra* were collected from Uhana, Ampara, Sri Lanka. High-purity Zinc Nitrate hexahydrate ($Zn(NO_3)_2 \cdot 6H_2O$) was procured from Loba Chemie Pvt. Ltd. Extra pure analytical reagent grade cupric sulfate ($CuSO_4 \cdot 5H_2O$, minimum purity 99.5%) was acquired from Sisco Research Laboratories Pvt. Ltd. Sodium hydroxide pellets (NaOH, minimum purity 98%) were sourced from Loba Chemie Pvt. Ltd. Anhydrous ferric chloride of analytical research grade ($FeCl_3$) was obtained from HiMedia Laboratories Pvt. Ltd. Potato Dextrose Agar (PDA) was purchased from HiMedia Laboratories Pvt. Ltd. Fusarium species were provided by the Plant Virus Indexing Centre in Homagama, Sri Lanka.

Preparation of the Mimosa Pigra Extract and Synthesis of ZnO NPs

M. pigra leaves were thoroughly washed with tap water and rinsed with DDW to remove all debris. The washed leaves were then dehydrated at 42°C for 24 hours, ground, and sieved to remove large particles. Eight grams of the dried leaf powder were mixed with 100 mL of DDW and stirred for 2 hours at 60°C and 400 rpm. The extract was centrifuged at 6000 rpm for 10 minutes, and the supernatant was filtered three times using Whatman No. 1 filter paper. Three grams of Zinc Nitrate hexahydrate ($Zn(NO_3)_2 \cdot 6H_2O$) were dissolved in 60 mL of the plant extract at room temperature and stirred for 1 hour. The solution was then heated in a thermal bath at 60°C for 12 hours to remove the water content. The resulting viscous paste was incubated at 100°C for 2 hours to form a crystalline powder-like material, which was subsequently calcined at 500°C for 2 hours.

Preparation of the Salvinia molesta extract and Synthesis of FeO NPs

S. molesta was thoroughly washed and dehydrated at 42°C for 24 hours. The dried plants were then ground and sieved to obtain a fine powder. Five grams of the powdered leaves were immersed in 80 mL of DDW and stirred for 1 hour at 60°C. The extract was filtered three times using Whatman No. 1 filter paper. This leaf extract was mixed with a pre-prepared 0.1 M $FeCl_3$ solution in a 2:3 ratio. The pH of the mixture was raised to 10 by incrementally adding 1 M sodium hydroxide. The reaction mixture was left undisturbed for 24 hours to facilitate the synthesis of FeO NPs. Subsequently, the mixture was centrifuged at 6000 rpm for 15 minutes, and the sediment was collected. The synthesized FeO NPs were washed trice with DDW and then calcined at 500°C for 2 hours. The resulting solid pellets were crushed using a mortar and pestle to obtain a fine powder-like structure.

Characterization Techniques

To verify the successful synthesis of ZnO, CuO, and FeO nanoparticles, UV-Visible (UV-Vis) spectroscopy analysis was conducted with a resolution of 1 nm over a range of 190 nm to 800 nm using a quartz cuvette. The morphology of the synthesized nanoparticles was inspected using Scanning Electron Microscopy (SEM). The SEM images were analyzed, and particle sizes were measured.

In Vitro Evaluation of Antifungal Activity on Mycelial Development

The antifungal activity of the nanoparticles against Fusarium species was assessed using the poisoned food technique. Potato dextrose agar (PDA) medium was prepared with nanoparticle suspensions at concentrations of 0 (negative control), 50, 100, 500, and 1000 mg/L, and Petri dishes (9 cm) were prepared with three replicates for each treatment. Agar discs (8 mm in diameter) containing mycelia of Fusarium species (7 days old, 28 ± 2°C) were then inoculated onto these plates. The plates were incubated at 28 ± 2°C until the fungal growth nearly covered the plate (9 cm). Mycelial growth was measured as diameter (mm). The percentage inhibition was calculated using the following formula (1):

$$\text{Inhibition percentage (\%)} = C\text{-}T/C \times 100 \quad (1)$$

Where "C" is the diameter of the fungal disc in the control, and "T" is the diameter of the fungal disc treated with different nanoparticle concentrations. Analysis of variance (ANOVA) was employed to determine significant differences between each mycelial growth treatment, with a 95% confidence interval ($\alpha = 0.05$) applied. Dunnett's test was used to identify differences between the means of the inhibition percentage data

compared to the control group. Duncan's Multiple Range Test (DMRT) was used to identify differences between the means of the inhibition percentage data for each treatment. The analysis was conducted using R statistical software (RStudio 2023.09.1+494).

RESULTS AND DISCUSSION

The synthesized nanoparticles (ZnO, CuO, and FeO) were characterized to confirm their successful synthesis and evaluate their properties. The UV-Vis spectroscopy analysis revealed distinct absorption peaks, indicative of

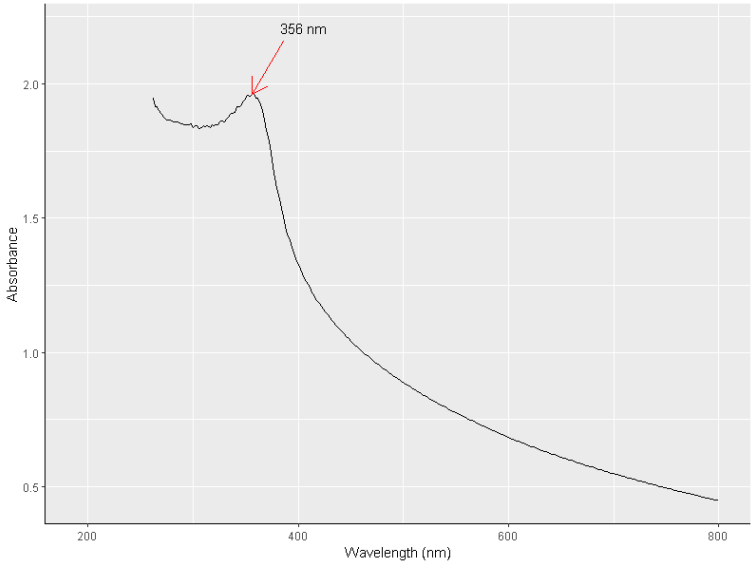

Figure 1: UV-Vis spectroscopy analysis of ZnO NPs

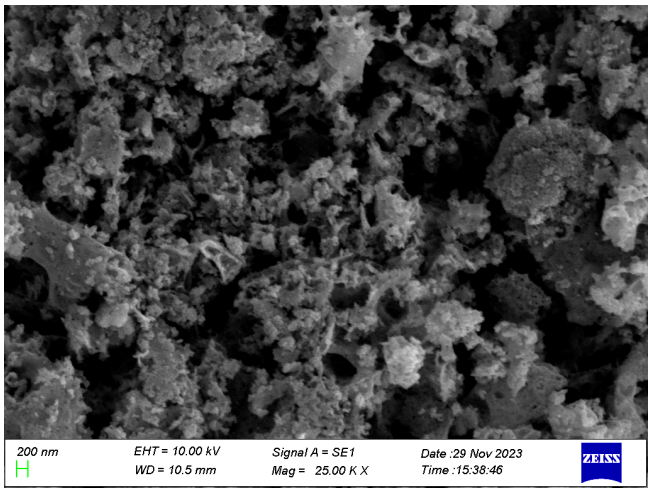

Figure 2: SEM images of ZnO NPs at a scale of 200 nm

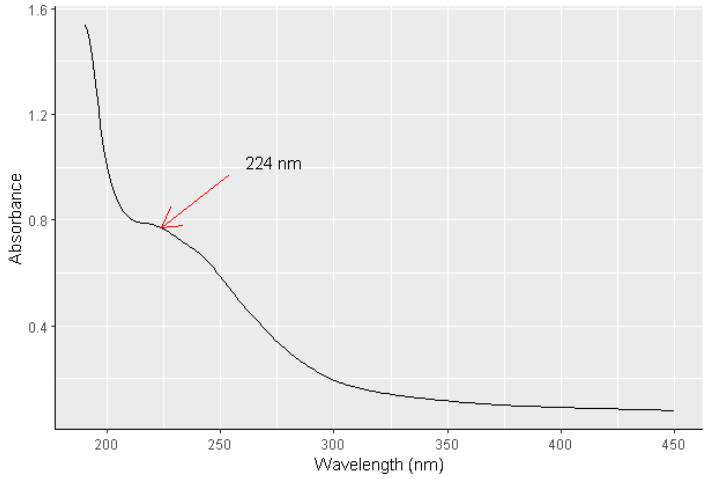

Figure 3: UV-Vis spectroscopy analysis of CuO NPs

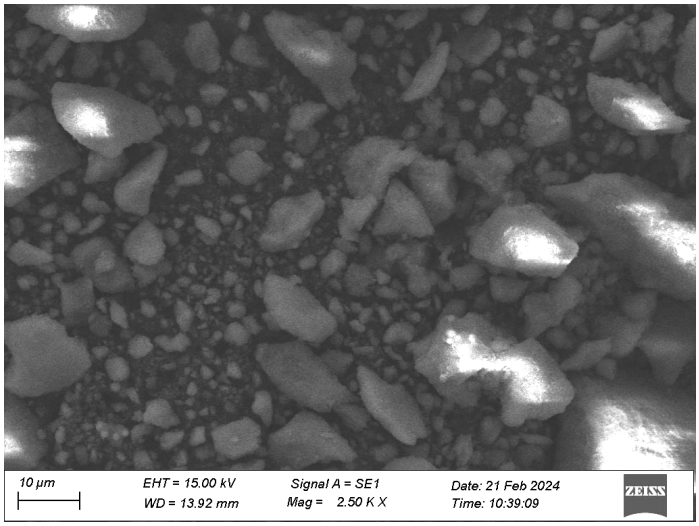

Figure 4: SEM images of CuO NPs at a scale of 10 µm

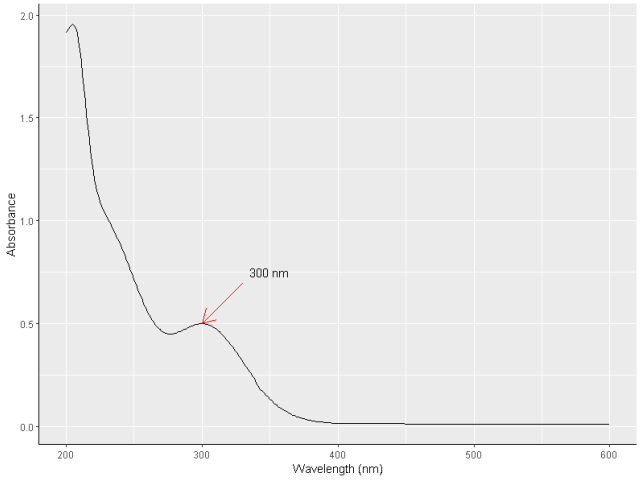

Figure 5: UV-vis spectroscopy analysis of FeO NPs

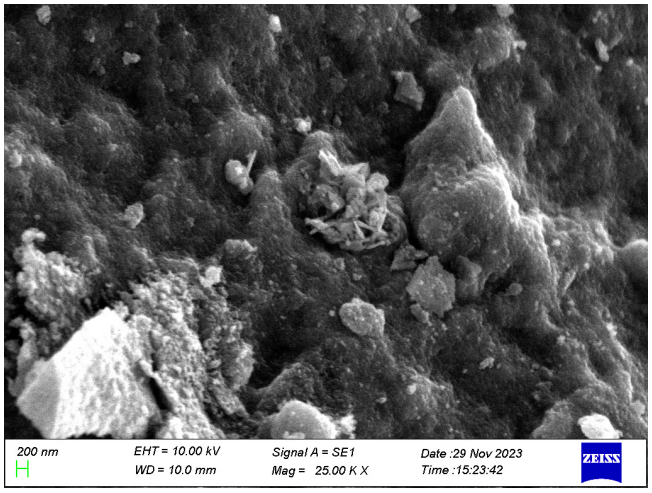

Figure 6: SEM images of FeO NPs at a scale of 200 nm

the formation of nanoparticles. The morphology and size of the nanoparticles were further analyzed using SEM.

Characterization of ZnO NPs

The green-synthesized ZnO NPs were characterized using UV-Vis spectroscopy with DMSO as a reference. Figure 1 shows a peak absorption at 356 nm, which preliminarily confirms the synthesis of ZnO NPs. The consistent result was observed in a previous study of Green synthesis of ZnO NPs using an aqueous extract of

Epipremnum aureum leaves photocatalytic degradation of Congo red having 326 as the maximum absorbance (Razia Sultana Brishti *et al.*, 2024). Another study of the synthesis of ZnO nanoparticles using peels of Passiflora foetida observed maximum absorbance at a wavelength ranging from 200 to 380 nm (Khan *et al.*, 2021). In a study on the green synthesis of ZnO-NPs using Juglans regia green husk aqueous extract, the biosynthesized ZnO-NPs exhibited a prominent maximum absorbance band at 360 nm, as indicated by the UV-Vis analysis results(Dehghani & Parinaz Ghadam, 2023). Collectively, these results affirm the successful production of ZnO NPs in the current study.

SEM images in Figure 2 reveal a heterogeneous distribution of shapes and sizes within the nanoscale range, with an average particle size of approximately 81 nm (35-164 nm). Consistent results have been reported for green-synthesized ZnO NPs with particle sizes of 30-100 nm (Thu *et al.*, 2022), 79 nm (Alyamani *et al.*, 2021), and 75-90 nm (Shanthi Sathappan *et al.*, 2021).

Characterization of CuO NPs

Maximum absorbance in the UV-Vis spectroscopy range of 190 nm to 450 nm was observed, with a peak at 224 nm, confirming the green synthesis of nanoparticles as shown in Figure 3. Similar results were reported in previous studies with absorption peaks at 265 nm (Kumar *et al.*, 2019), 220 nm (Renuga *et al.*, 2020), and 250–255 nm (Kumar *et al.*, 2017).

The SEM images illustrated in Figure 04 reveal CuO NPs with diverse shapes and sizes, averaging approximately 108 nm in diameter, and show a tendency to aggregate and form various structures. Consistent results were also obtained in previous studies, reporting particle sizes of 18-106 nm (Selvi *et al.*, 2019), 197 nm (Arushi Saloki & Daharwal, 2023), and 20-200 nm (Manivannan Rangasamy *et al.*, 2023).

Characterization of FeO NPs

UV-Vis spectrometry indicated the formation of green-synthesized nanoparticles within the range of 200 to 600 nm, with a maximum absorbance at 300 nm, confirming the synthesis of FeO NPs. Consistent results were also observed in previous studies, with maximum absorbance at 295–301 nm (Karpagavinayagam & Vedhi, 2019), 293 nm (Andrade-Zavaleta *et al.*, 2022), and 230 and 290 nm (Hussain *et al.*, 2023).

SEM images in Figure 6 show the shapes and sizes of the iron oxide nanoparticles, which exhibit a variety of nanoscale shapes and sizes, averaging around 82 nm (ranging from 41 to 140 nm), and tend to clump together and form multiple structures. Similar results were also observed having particle sizes 30–100 nm (Karpagavinayagam & Vedhi, 2019), and 88 nm (Aigbe & Osibote, 2024).

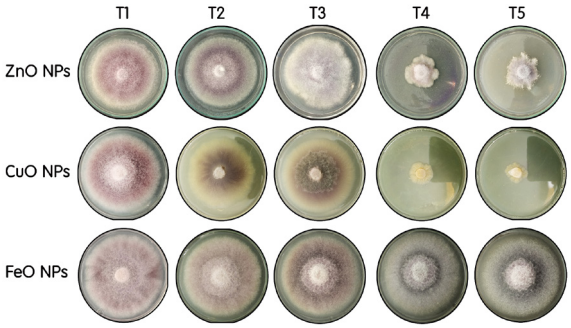

Figure 7: *Rhizoctonia* species mycelial growth inhibition test treated with NPs synthesized by the green route: FeO NPs; (T1) 0 mg/L, (T2) 50 mg/L, (T3) 100 mg/L, (T4) 500 mg/L, (T5) 1000 mg/L

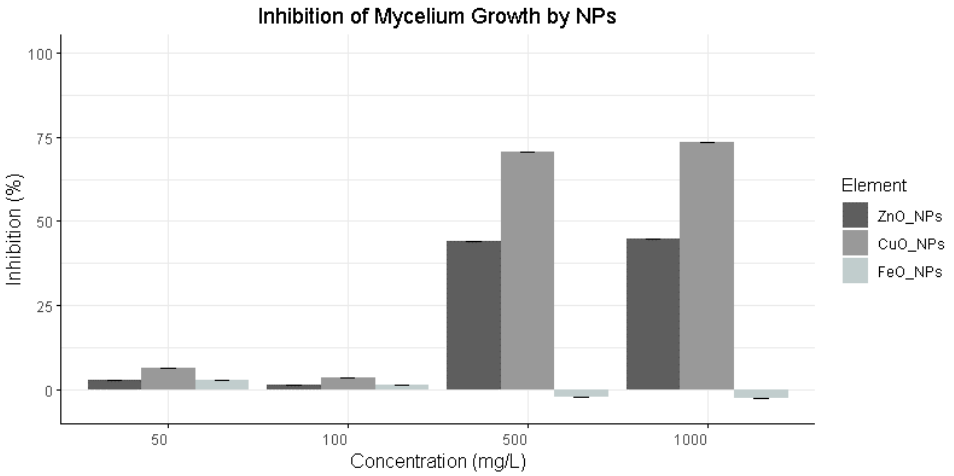

Figure 8: Mycelium growth inhibition % of *Rhizoctonia* species by different nanoparticles

Evaluation of the Antifungal Effect of the NPs

The antifungal effect on mycelial growth of the synthesized nanoparticles was evaluated by amending the culture medium with different NP concentrations and recording the fungus colony diameter over 7-9 days until the fungus nearly covered the plate (9 cm), with one nanoparticle tested at a time. All tested NPs varied in their extent of inhibition of *Rhizoctonia* species colony growth at different concentrations, with statistically significant differences calculated among the nanoparticles. As illustrated in Figure 7, the inhibition of *Rhizoctonia* species colony growth was observed.

Table 1: Inhibition of colony growth of *Rhizoctonia* Species over control by poisoned food technique treated with ZnO NPs

Concentration (mg/L)	Diameter (mm)	Colony growth inhibition %	DMRT test result
0	80.03 ± 0.59		a
50	77.7 ± 4.64	2.91%	a
100	78.9 ± 3.31	1.41%	a
500	44.77 ± 7.17	44.06%	b
1000	44.23 ± 8.21	44.73%	b

Each value is mean of 3 replicates ± SD

ZnO NPs affected the mycelium growth at different concentrations, as tabulated in Table 1. The one-way ANOVA analysis demonstrated significant differences among the treatment groups, with a p-value (Pr > F) of less than 0.001 and an F value of 35.14. This indicates that the variation in mycelial growth among the different nanoparticle concentrations is statistically significant. The control group (0 mg/L) exhibited a *Rhizoctonia* mycelium growth diameter of 80.03 ± 0.59 mm. For the 50 and 100 mg/L concentrations, the mycelium growth diameters were 77.7 ± 4.64 mm and 78.9 ± 3.31 mm, respectively. According to Dunnett's test, there was no significant difference between the 0, 50, and 100 mg/L groups, despite inhibition percentages of 2.91% and 1.41% for the 50 and 100 mg/L concentrations, respectively.

In contrast, the FeO NPs at higher concentrations (500 and 1000 mg/L) exhibited significant inhibition of mycelium growth compared to the control. The mycelium growth diameters for the 500 and 1000 mg/L concentrations were 44.77 ± 7.17 mm and 44.23 ± 8.21 mm, respectively. The inhibition percentages for these concentrations were substantially higher, at 44.06% for the 500 mg/L concentration and 44.73% for the 1000 mg/L concentration. These results indicate that higher concentrations of ZnO NPs are more effective in inhibiting *Rhizoctonia* mycelium growth.

Previous studies have also demonstrated the dose-dependent effect of ZnO NPs on the inhibition of *Rhizoctonia* mycelium growth. For example, Jannat *et al.* (2022) reported inhibition percentages of 17.1%, 31%, 40%, 48.7%, and 51.1% for *R. solani* at ZnO NP concentrations of 0.05, 0.15, 0.25, 0.35, and 0.45 mg/mL, respectively. In another study, green-synthesized ZnO NPs exhibited significant growth inhibition of *R. solani*, with inhibition percentages of 70.2 ± 0.5%, 61.4 ± 0.5%, 48.5 ± 0.5%, 1.2 ± 0.5%, and 0.6 ± 0.5% at concentrations of 1.0, 0.75, 0.5, 0.25, and 0.1 mg/mL, respectively (Ali *et al.*, 2022). Those previous findings also support the dose-dependent manner of ZnO NPs inhibition of *Rhizoctonia* mycelium growth.

Table 2: Inhibition of colony growth of *Rhizoctonia* Species over control by poisoned food technique treated with CuO NPs

Concentration (mg/L)	Diameter (mm)	Colony growth inhibition %	DMRT test result
0	78.24 ± 1.25		a
50	73.38 ± 2.07	6.21%	a
100	75.60 ± 3.58	3.37%	a
500	22.97 ± 0.67	70.64%	b
1000	20.79 ± 2.75	73.43%	b

Each value is mean of 3 replicates ± SD

The one-way ANOVA analysis demonstrated significant differences among the treatment groups of different concentrations of CuO NPs, with a p-value (Pr > F) of less than 0.001 and an F value of 494.5. Table 2 illustrates the dose-dependent effect of CuO NPs on inhibiting the mycelium growth of *Rhizoctonia* species. The control group exhibited a mycelium diameter of 78.24 ± 1.25 mm. At concentrations of 50 mg/L and 100 mg/L, the mycelium diameters were 73.38 ± 2.07 mm and 75.60 ± 3.58 mm, respectively, which were statistically similar to the control group (Duncan's Multiple Range Test, DMRT), with growth inhibitions of 6.21% and 3.37%.

In contrast, concentrations of 500 mg/L and 1000 mg/L resulted in mycelium diameters of 22.97 ± 0.67 mm and 20.79 ± 2.75 mm, respectively. These values were statistically similar to each other (DMRT) but significantly

different from the control group (Dunnett's test), showing inhibitions of 70.64% and 73.43%, respectively. These results indicate that higher concentrations of CuO NPs are more effective in inhibiting *Rhizoctonia* mycelium growth.

Previous study also suppor the findgs as at 150 ppm the CuO NPs synthesized by chemical reduction method could inhibit the growth of *R. solani* by 62% (Chowdhury *et al.*, 2024). Another study of green synthesized CuO NPs in the concentrations of 50,100, and 200 ppm , maximum inhibition was recorded in 200ppm having 11.89% inhibition of *R. solani*(Fetyan *et al.*, 2024). Similar study of CuO-NPs biosynthesized from *H. bacciferum* leaf extract and antifungal activity for *R. solani* by 20, 50, 75, and 100 µg/mL they observed inhibition of mycelium growth 81.48% inhibition in 100 µg/mL concentration (Hamdy *et al.*, 2024).

Table 3: Inhibition of colony growth of *Rhizoctonia* Species over control by poisoned food technique treated with FeO NPs

Concentration (mg/L)	Diameter (mm)	Colony growth inhibition %
0	80.53 ± 1.28	
50	78.2 ± 3.54	2.89%
100	79.54 ± 0.63	1.23%
500	82.33 ± 2.06	-2.24%
1000	82.71 ± 0.60	-2.71%

Each value is mean of 3 replicates ± SD

The one-way ANOVA analysis indicated no significant differences in the mean radial growth of *Rhizoctonia* mycelium treated with FeO NPs (F value: 2.81, Pr > F > 0.05). The control and all treatments showed no significant differences, though minor inhibition and promotion zones were observed compared to the control. The maximum inhibition occurred at 50 mg/L, while the minimum inhibition was observed at 1000 mg/L. Similar results were found in a study on the effects of FeO NPs on the mycelial growth of rot-causing fungi, where treatments with 0.1, 0.25, and 0.5 mg/mL resulted in mycelial growth of 12.00 ± 1.00 mm, 14.33 ± 0.57 mm, and 16.33 ± 0 mm, respectively, indicating higher concentrations led to increased growth rather than inhibition. Many results found in the literature do not align with the observed data. For instance, a previous study reported significant inhibition of mycelium growth at various concentrations of FeO NPs. Specifically, FeO NPs showed highly significant growth reduction, with the maximum growth inhibition (87.9%) observed at a concentration of 1.0 mg/mL (Ali *et al.*, 2020). Another study investigated the growth inhibition percentages of different concentrations of iron oxide nanoparticles against two tested *A. alternata* strains. They observed mycelium inhibition at 29.85%, 47.24%, 55.95%, 65.74%, and 75.89% for concentrations of 50, 100, 200, 400, and 800 ppm, respectively (Yassin *et al.*, 2023).

Figure 8 illustrates that different concentrations of nanoparticles and various types of nanoparticles inhibit mycelium growth of *Rhizoctonia* species in a dose-dependent manner. The maximum inhibition was observed with CuO NPs at 500 and 1000 mg/L, followed by ZnO NPs. The FeO NPs did not inhibit the *Rhizoctonia* mycelium at higher concentrations, and instead promoted growth to a minor extent, although this increase was not statistically significant. The inhibition of mycelium growth by nanoparticles in a dose-dependent manner can be attributed to various mechanisms. For instance, NPs may cause cell membrane damage, leading to increased membrane permeability. This disruption can induce responses within intracellular organelles, potentially altering DNA and RNA through mutation, affecting ion transport pathways, and disrupting protein functions (Foldbjerg *et al.*, 2015). Smaller nanoparticles, as suggested by Gliga *et al.* (2014), possess a larger surface area relative to their volume, facilitating easier penetration of fungal cell walls and membranes. This penetration can trigger responses within intracellular organelles. Nanoparticles are also known to generate reactive oxygen species, which can further alter fungal membrane permeability. This alteration compromises cell structure and leads to osmotic imbalance, affecting fungal functions (Kumari *et al.*, 2019). Studies have shown that silver nanoparticles inhibit spore germination in B. cinerea in a concentration-dependent manner (Bayat *et al.*, 2021). Despite these insights, the mechanisms by which green-synthesized nanoparticles affect mycelium growth inhibition remain incompletely understood. Further research is necessary to fully assess the potential impacts of nanomaterials on altering fungal growth dynamics.

CONCLUSION

The current study successfully synthesized ZnO, CuO, and FeO nanoparticles using a cost-effective and environmentally friendly procedure. The synthesized nanoparticles were characterized by UV-Vis spectroscopy and SEM analysis. The antifungal activity of the synthesized nanoparticles was evaluated at different concentrations using the poison food technique, testing one nanoparticle at a time. The results indicate that both ZnO and CuO nanoparticles exhibit a dose-dependent effect on mycelium growth inhibition, with higher concentrations (500 and 1000 mg/L) causing significant inhibition compared to the untreated *Rhizoctonia* species.

In contrast, FeO nanoparticles did not exhibit dose-dependent inhibition of mycelium growth but caused minor promotion, which was not statistically significant. The study concludes that among ZnO, CuO, and FeO nanoparticles, CuO nanoparticles at a concentration of 1000 mg/L demonstrated the maximum inhibition, followed by ZnO nanoparticles. The observed variations in mycelium inhibition by different nanoparticles at various concentrations highlight the complexity of nanoparticle interactions with fungal pathogens, underscoring the need for further research to optimize their antifungal efficacy.

Funding

Competitive Research Grant 2020, Grant Number 202003, The Open University of Sri Lanka.

Declaration of Generative AI and AI-Assisted Technologies in the Writing Process

During the preparation of this work, the authors used ChatGPT 3.5 to improve language and readability. After using this tool/service, the authors reviewed and edited the content as needed and take full responsibility for the content of the publication.

REFERENCES

Aigbe, U. O., & Osibote, O. A. (2024). Green Synthesis of Metal Oxide Nanoparticles, and Their Various ApAigbe, U. O., & Osibote, O. A. (2024). Green Synthesis of Metal Oxide Nanoparticles, and Their Various Applications. *Journal of Hazardous Materials Advances, 13,* 100401–100401. https://doi.org/10.1016/j.hazadv.2024.100401

Ali, M., Haroon, U., Khizar, M., Chaudhary, H. J., & Munis, M. F. H. (2020). Facile single step preparations of phyto-nanoparticles of iron in Calotropis procera leaf extract to evaluate their antifungal potential against Alternaria alternata. *Current Plant Biology, 23,* 100157. https://doi.org/10.1016/j.cpb.2020.100157

Ali, M., Wang, X., Haroon, U., Chaudhary, H. J., Kamal, A., Ali, Q., Saleem, M. H., Usman, K., Alatawi, A., Ali, S., & Hussain Munis, M. F. (2022). Antifungal activity of Zinc nitrate derived nano Zno fungicide synthesized from Trachyspermum ammi to control fruit rot disease of grapefruit. *Ecotoxicology and Environmental Safety, 233,* 113311. https://doi.org/10.1016/j.ecoenv.2022.113311

Alyamani, A. A., Albukhaty, S., Aloufi, S., AlMalki, F. A., Al-Karagoly, H., & Sulaiman, G. M. (2021). Green Fabrication of Zinc Oxide Nanoparticles Using Phlomis Leaf Extract: Characterization and In Vitro Evaluation of Cytotoxicity and Antibacterial Properties. *Molecules, 26*(20), 6140. https://doi.org/10.3390/molecules26206140

Andrade-Zavaleta, K., Chacon-Laiza, Y., Asmat-Campos, D., & Raquel-Checca, N. (2022). Green Synthesis of Superparamagnetic Iron Oxide Nanoparticles with Eucalyptus globulus Extract and Their Application in the Removal of Heavy Metals from Agricultural Soil. *Molecules, 27*(4), 1367. https://doi.org/10.3390/molecules27041367

Saloki, A., & Daharwal, S. J. (2023). Green synthesis of copper oxide nanoparticle from plant extract and its antibacterial activity. *Asian Journal of Pharmaceutical and Clinical Research, 16*(7), 172–176. https://doi.org/10.22159/ajpcr.2023.v16i7.47122

Bayat, M., Zargar, M., Chudinova, E., Astarkhanova, T., & Pakina, E. (2021). In vitro evaluation of antibacterial and antifungal activity of biogenic silver and copper nanoparticles: The first report of applying biogenic nanoparticles against *Pilidium concavum and Pestalotia sp. fungi. Molecules, 26*(17), 5402. https://doi.org/10.3390/molecules26175402

Chaube, H. S., & Pundhir, V. S. (2005). *Crop diseases and their management.* PHI Learning Pvt. Ltd. https://shorturl.at/btxtU

Chowdhury, A. R., Kumar, R., Mahanty, A., Mukherjee, K., Kumar, S., Tribhuvan, K. U., Sheel, R., Lenka, S., Singh, B. K., Chattopadhyay, C., Sharma, T. R., Bhadana, V. P., & Sarkar, B. (2019). Inhibitory role of copper and silver nanocomposite on important bacterial and fungal pathogens in rice (Oryza sativa). *Scientific Reports, 14*(1), 1779. https://doi.org/10.1038/s41598-023-49918-0

Dehghani, M., & Ghadam, P. (2023). Green synthesis of ZnO-NPs by *Juglans regia* green husk aqueous extract. https://doi.org/10.3390/iocn2023-14444

Durgeshlal, C., Sahroj Khan, M., Prabhat, S. A., & Aaditya Prasad, Y. (2019). Antifungal Activity of Three Different Ethanolic Extract against Isolates from Diseased Rice Plant. *Journal of Analytical Techniques and Research, 01*(01). https://doi.org/10.26502/jatri.007

Dutta, P., Kumari, A., Madhusmita Mahanta, Gunadhya Kr Upamanya, Punabati Heisnam, Sarodee Borua, Pranjal Kr Kaman, Awdhesh Kumar Mishra, Mallik, M., Gomathy Muthukrishnan, Sabarinathan, K. G., Krishti Rekha Puzari, & Dumpapenchala Vijayreddy. (2023). Nanotechnological approaches for management of soil-borne plant pathogens. *Frontiers in Plant Science, 14*. https://doi.org/10.3389/fpls.2023.1136233

Fetyan, N. A. H., Essa, T. A., Salem, T. M., Taha, A. A., Elgobashy, S. F., Tharwat, N. A., & Elsakhawy, T. A. M. R. D. (2024). Promising eco-friendly nanoparticles for managing bottom rot disease in lettuce (Lactuca sativa var. longifolia). *Microbiology Research, 15*(1), 14. https://doi.org/10.3390/microbiolres15010014

Foldbjerg, R., Jiang, X., Miclăuş, T., Chen, C., Autrup, H., & Beer, C. (2015). Silver nanoparticles – wolves in sheep's clothing? *Toxicology Research, 4*(3), 563–575. https://doi.org/10.1039/c4tx00110a

Gliga, A. R., Skoglund, S., Odnevall Wallinder, I., Fadeel, B., & Karlsson, H. L. (2014). Size-dependent cytotoxicity of silver nanoparticles in human lung cells: the role of cellular uptake, agglomeration and Ag release. *Particle and Fibre Toxicology, 11*(1), 11.

https://doi.org/10.1186/1743-8977-11-11

Hamdy, E., Hamada El-Gendi, Abdulaziz Al-Askar, El-Far, A., Przemysław Kowalczewski, Said Behiry, & Abdelkhalek, A. (2024). Copper oxide nanoparticles-mediated Heliotropium bacciferum leaf extract: Antifungal activity and molecular docking assays against strawberry pathogens. *Open Chemistry, 22*(1). https://doi.org/10.1515/chem-2024-0028

Hussain, A., Yasar, M., Ahmad, G., Ijaz, M., Aziz, A., Nawaz, M. G., Khan, F. A., Iqbal, H., Shakeel, W., Momand, H., Ali, R., Ahmad, S., Shah, H., Nadeem, M., Ahmad, D., Anjum, F., & Faisal, S. (2023). Synthesis, characterization, and applications of iron oxide nanoparticles. *International Journal of Health Sciences, 17*(4), 3–10. https://www.ncbi.nlm.nih.gov/pmc/articles/PMC10321464/

Jaiswal, A. K., Elad, Y., Graber, E. R., & Frenkel, O. (2014). *Rhizoctonia* solani suppression and plant growth promotion in cucumber as affected by biochar pyrolysis temperature, feedstock and concentration. *Soil Biology and Biochemistry, 69,* 110–118. https://doi.org/10.1016/j.soilbio.2013.10.051

Jannat, M., Kiran, S., Yousaf, S., Gulzar, T., & Iqbal, S. (2022). Potential Antifungal Effects of D. malabarica Assisted Zinc Oxide and Silver Nanoparticles against Sheath Blight Disease of *Rhizoctonia* solani. *Polish Journal of Environmental Studies, 31*(5). https://doi.org/10.15244/pjoes/150049

Jeevanandam, J., Barhoum, A., Chan, Y. S., Dufresne, A., & Danquah, M. K. (2018). Review on Nanoparticles and Nanostructured materials: history, sources, Toxicity and Regulations. *Beilstein Journal of Nanotechnology, 9*(1), 1050–1074. https://doi.org/10.3762/bjnano.9.98

Karkee, A., & Mandal, D. L. (2020). Efficacy of Fungicides Against *Rhizoctonia* solani Inciting Rhizome Rot Diseases on Large Cardamom (Amomum subulatum Roxb.). *International Journal of Applied Sciences and Biotechnology, 8*(1), 61–64. https://doi.org/10.3126/ijasbt.v8i1.27240

Karpagavinayagam, P., & Vedhi, C. (2019). Green synthesis of iron oxide nanoparticles using Avicennia marina flower extract. *Vacuum, 160,* 286–292. https://doi.org/10.1016/j.vacuum.2018.11.043

Khan, M., Ware, P., & Shimpi, N. (2021). Synthesis of ZnO nanoparticles using peels of Passiflora foetida and study of its activity as an efficient catalyst for the degradation of hazardous organic dye. *SN Applied Sciences, 3*(5). https://doi.org/10.1007/s42452-021-04436-4

Kumar, B., Smita, K., Cumbal, L., Debut, A., & Angulo, Y. (2017). Biofabrication of copper oxide nanoparticles using Andean blackberry (Rubus glaucus Benth.) fruit and leaf. *Journal of Saudi Chemical Society, 21,* S475–S480. https://doi.org/10.1016/j.jscs.2015.01.009

Kumar, P., Nene, A. G., Punia, S., Kumar, M., Abbas, Z., Thakral, F., & Tuli, H. S. (2019). Synthesis, characterization, and antibacterial activity of CuO nanoparticles. *International Journal of Applied Pharmaceutics, 12*(1), 17–20. https://doi.org/10.22159/ijap.2020v12i1.36271

Kumari, M., Giri, V. P., Pandey, S., Kumar, M., Katiyar, R., Nautiyal, C. S., & Mishra, A. (2019). An insight into the mechanism of antifungal activity of biogenic nanoparticles than their chemical counterparts. *Pesticide Biochemistry and Physiology, 157,* 45–52. https://doi.org/10.1016/j.pestbp.2019.03.005

Manivannan Rangasamy, Suresh Kumar Gopal, A. Indhumathi, S. Loganathan, S. Manikandan, & R. Naresh. (2023). Green Synthesis and Characterization of Copper Oxide Nanoparticles Using Tecoma Stans. *Journal of Pharmaceutical Research International, 35*(7), 9–16. https://doi.org/10.9734/jpri/2023/v35i77335

Moliszewska, E., Hendel, P., & Małgorzata Nabrdalik. (2023). *Rhizoctonia* spp. as beneficial and mycorrhizal fungi. *Elsevier EBooks,* 213–220. https://doi.org/10.1016/b978-0-323-91734-6.00004-1

Mousa, S., Abdulwahab, J., & Abdulhai, M. (2024). Isolation and Pathogenicity Testing of Potato Varieties' Susceptibility to the Fungus *Rhizoctonia* solani Kuhn in Northern Syria. *African Journal of Biological Sciences, 6,* 1569–1578. https://doi.org/10.33472/AFJBS.6.8.2024.15691578

Razia Sultana Brishti, Md. Ahsan Habib, Mosummath Hosna Ara, Karim, R., Md. Khairul Islam, Jannatul Naime, Hasan, M., & Abu, M. (2024). Green synthesis of ZnO NPs using aqueous extract of Epipremnum aureum leave: Photocatalytic degradation of Congo red. *Results in Chemistry, 7,* 101441–101441. https://doi.org/10.1016/j.rechem.2024.101441

Renuga, D., Jeyasundari, J., Shakthi Athithan, A. S., & Brightson Arul Jacob, Y. (2020). Synthesis and characterization of copper oxide nanoparticles using Brassica oleracea var. italic extract for its antifungal application. *Materials Research Express, 7*(4), 045007. https://doi.org/10.1088/2053-1591/ab7b94

Selvi, V. S., Velumani, A., & Banu, N. N. (2019). Synthesis and characterization of copper oxide nanoparticles (CuO NPs) using Mangifera indica leaf extract. *Journal of Nanoscience and Technology, 5*(4), 784–786. https://doi.org/10.30799/jnst.240.19050411

Sathappan, S., Kirubakaran, N., Gunasekaran, D., Gupta, P., Verma, R. S., & Janarthanan, S. (2021). Green synthesis of zinc oxide nanoparticles (ZnO NPs) using Cissus quadrangularis: Characterization, antimicrobial, and anticancer studies. *Proceedings of the National Academy of Sciences, India, Section B: Biological Sciences, 91*(2), 289–296. https://doi.org/10.1007/s40011-020-01215-w

Sharma, A., Kumar, V., Shahzad, B., Tanveer, M., Sidhu, G. P. S., Handa, N., Kohli, S. K., Yadav, P., Bali, A. S., Parihar, R. D., Dar, O. I., Singh, K., Jasrotia, S., Bakshi, P., Ramakrishnan, M., Kumar, S., Bhardwaj, R., & Thukral, A. K. (2019). Worldwide pesticide usage and its impacts on ecosystem. *SN Applied Sciences, 1*(11), Article 1485. https://doi.org/10.1007/s42452-019-1485-1

Thu, T., Nguyen Duy Dat, Tam, L.-M., & Nguyen Hoang Phuong. (2022). Green synthesis of zinc oxide nanoparticles toward highly efficient photocatalysis and antibacterial application. *Beilstein Journal of Nanotechnology, 13,* 1108–1119. https://doi.org/10.3762/bjnano.13.94

Tsror, L. (2010). Biology, Epidemiology and Management of *Rhizoctonia* solani on Potato. *Journal of Phytopathology, 158*(10), 649–658. https://doi.org/10.1111/j.1439-0434.2010.01671.x

Tu, C., Hsieh, T., & Chang, Y. (1996). Vegetable diseases incited by *Rhizoctonia* spp. In *Fungal diseases in plants* (pp. 369–377). Springer. https://doi.org/10.1007/9789401729017_34

Yassin, M. T., Al-Otibi, F. O., Al-Askar, A. A., & Alharbi, R. I. (2023). Green Synthesis, Characterization, and Antifungal Efficiency of Biogenic Iron Oxide Nanoparticles. *Applied Sciences, 13*(17), 9942. https://doi.org/10.3390/app13179942plications. Journal of Hazardous Materials Advances, 13, 100401–100401. https://doi.org/10.1016/j.hazadv.2024.100401